

THE PROCESSING OF HYPERBOLOID SURFACES USING WIRE ELECTRICAL DISCHARGE MACHINING – PRACTICAL ASPECTS

Călin Denes¹

¹ "Lucian Blaga" University of Sibiu, Romania, 550 024 Sibiu, 10 Victoriei Blvd., Romania, phone: +40 742 411 863;
fax: +40 269 218153, calin.denes@ulbsibiu.ro

ABSTRACT: The paper presents practical aspects of an original method that can be used for cutting hyperboloid surfaces using wire electrical discharge machining (WEDM). The processing method, which has only been partly revealed by the author in certain relatively low-impact Romanian publications, is now fully delineated in the form of two papers that focus on both the theoretical and practical aspects of the processing of hyperboloid surfaces using wire electrical discharge machining. This paper presents the practical aspects of the method of generating hyperboloid surfaces. The numerical and geometric simulation of the generation of hyperboloid surfaces using wire electrical discharge machining is shown, together with the way of programming the processing, certain technological limitations regarding the processing of hyperboloid surfaces, and real-world conclusions concerning the generation of surfaces being processed via wire electrical discharge machining.

KEY WORDS: WEDM, hyperboloid surfaces, theoretical and practical aspects

1. GENERALITIES

Papers [1] and [2] present the theoretical aspects regarding the generation of hyperboloid surfaces via wire electrical discharge machining. In order to generate a hyperboloid surface in the shape of a hyperboloid of revolution, whose height is $H = 2 \cdot h$ and whose axial profile is defined by the equilateral hyperbola [H], similar to the one shown in Figure 1, the wire electrode must first occupy position Mm_1 .

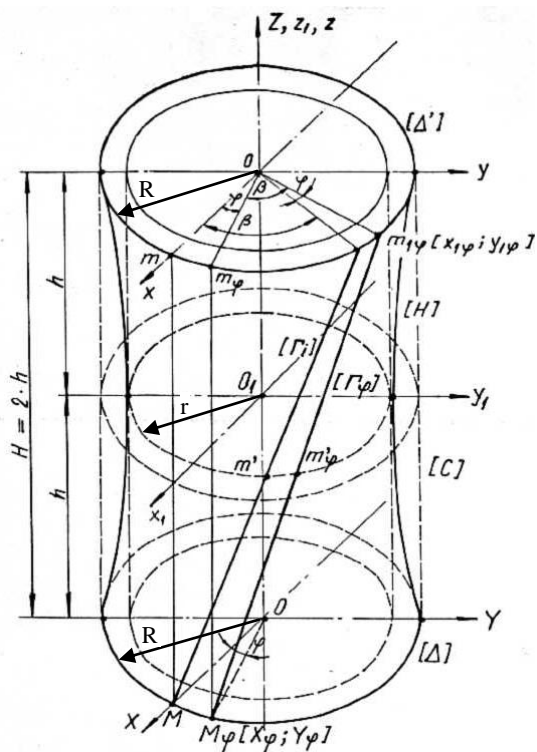


Figure 1. Generating a hyperboloid surface

By revolving the wire electrode about vertical axis Oo at an angle $\varphi \in [0, 2\pi]$, we obtain the hyperboloid surface defined by the ends, whose upper and lower circle are of radius $R = om = OM$ and the middle, whose collar circle is of radius $r = O_1m'$. If the wire electrode is maintained in a vertical position at all times and is rotated about Mm at $\varphi \in [0, 2\pi]$, what results is a cylindrical surface whose height is $H=2 \cdot h$ and whose radius is $OM = om = R$.

Globally speaking, there has only been one mention regarding the processing of such surfaces [2]; however, no practical explanations are given on the way in which the processing can be done. Due to this, a research into the mechanism of generation of these surfaces, complete with the theoretical grounding of the process, as well as its practical implementation, are more than welcome.



Figure 2. Hyperboloid surfaces processed using wire electrical discharge machining

Figure 2 presents sample hyperboloid surfaces achieved using wire electrical discharge machining, as shown in Figure 3. The only explanation that is needed is that the processing was carried out by slanting the wire electrode and having it occupy consecutive positions, as shown in Figure 1. The parts obtained feature both outer and inner hyperboloid surfaces, the outer ones being only partly processed, so as to maintain a connection with the workpiece's material.

2. SIMULATING THE GENERATION OF HYPERBOLOID SURFACES

In order to validate the theory concerning the generation of hyperboloid surfaces via WEDM, a simulation was carried out generating these surfaces by revolving the wire electrode as shown in Figure 1 (together with the accompanying explanations). To

do this, based on the mathematical apparatus outlined in paper [2], the applications used were MS-Excel, for the numerical simulation, and Kovoprog III, a specialized application, for the graphical simulation. The latter is used specifically to program WEDM machinery by a manufacturing company from Sibiu.

Regarding the MS-Excel application, a worksheet called "hiperboloid_electrod_mobil.xls" was used. This contains two sheets: the first (Figure 3) is used to calculate the endpoints of the generating curve $[\Gamma]$ ($M[X,Y]$ and $m_1[x,y]$), according to the notations used in Figure 1; the second (Figure 4) illustrates the laws of motion of these two points along the two generating curves: upper $[\Delta']$ and lower $[\Delta]$ – see Figure 1.

Microsoft Excel - hiperboloid_electrod_mobil.xls

File Edit View Insert Format Tools Data Window Help

Arial 10 B I U Σ $f(x)$ Δ Δ 100% \mathbb{C}

F4 = =C4*A4/SQRT(B4^2-A4^2)

	A	B	C	D	E	F	G	H	I	J	K
1	Date initiale			Calcule semiaxe hiperbolă generatoare							
2											
3	r	R	h		a	b	c				
4	15	20	30		15	34.0168	37.17718				
5											
6	Calcul date intermediiare										
7											
8	H	beta [rad]	BETA		beta [grade]						
9	60	1.445468	1.445468496		82.81924						
10											
11	Calcul pozitiilor semnificative										
12											
13	fi	X(fi)	Y(fi)	x(fi)	y(fi)		fi	X(fi)	Y(fi)	x(fi)	y(fi)
14	0	20	0	2.5	19.84313		1.57	0.015927	19.99999	-19.8411	2.515801
15	0.785398	14.14214	14.14213562	-12.2634	15.79898						
16	1.570796	1.23E-15	20	-19.8431	2.5						
17	2.356194	-14.1421	14.14213562	-15.799	-12.2634						
18	3.141593	-20	2.4503E-15	-2.5	-19.8431						
19	3.926991	-14.1421	-14.14213562	12.26345	-18.6821						
20	4.712389	-3.7E-15	-20	19.84313	-2.5						
21	5.497787	14.14214	-14.14213562	15.79898	12.26345						
22	6.283185	20	-4.90059E-15	2.5	19.84313						
23											
24											

Sheet1 / Sheet2 / Sheet3 /

Ready

Start Microsoft Excel - hipe... hiperboloidal1.doc - Micros... 5:09 PM

Figure 3. Numerical simulation calculi for the wire electrode

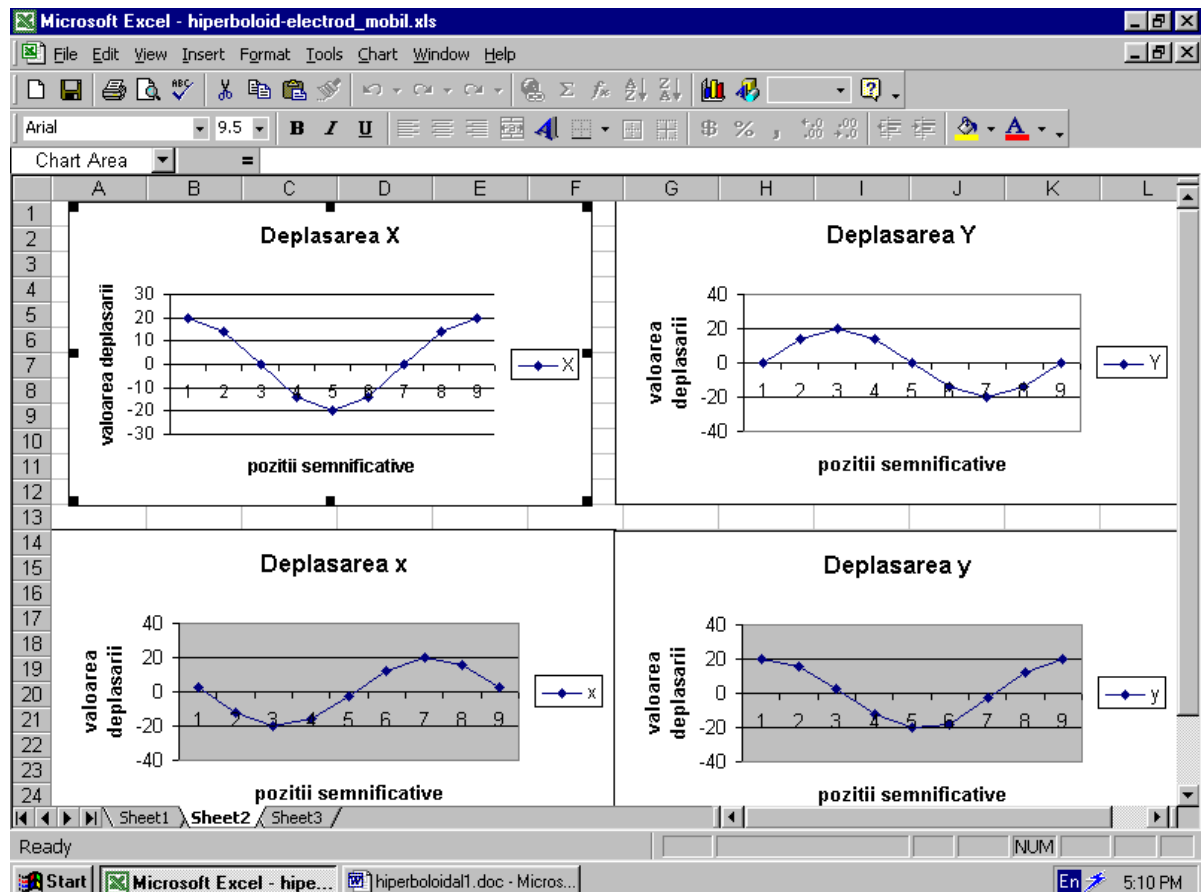


Figure 4. The laws of motion of the slanted and mobile wire electrode

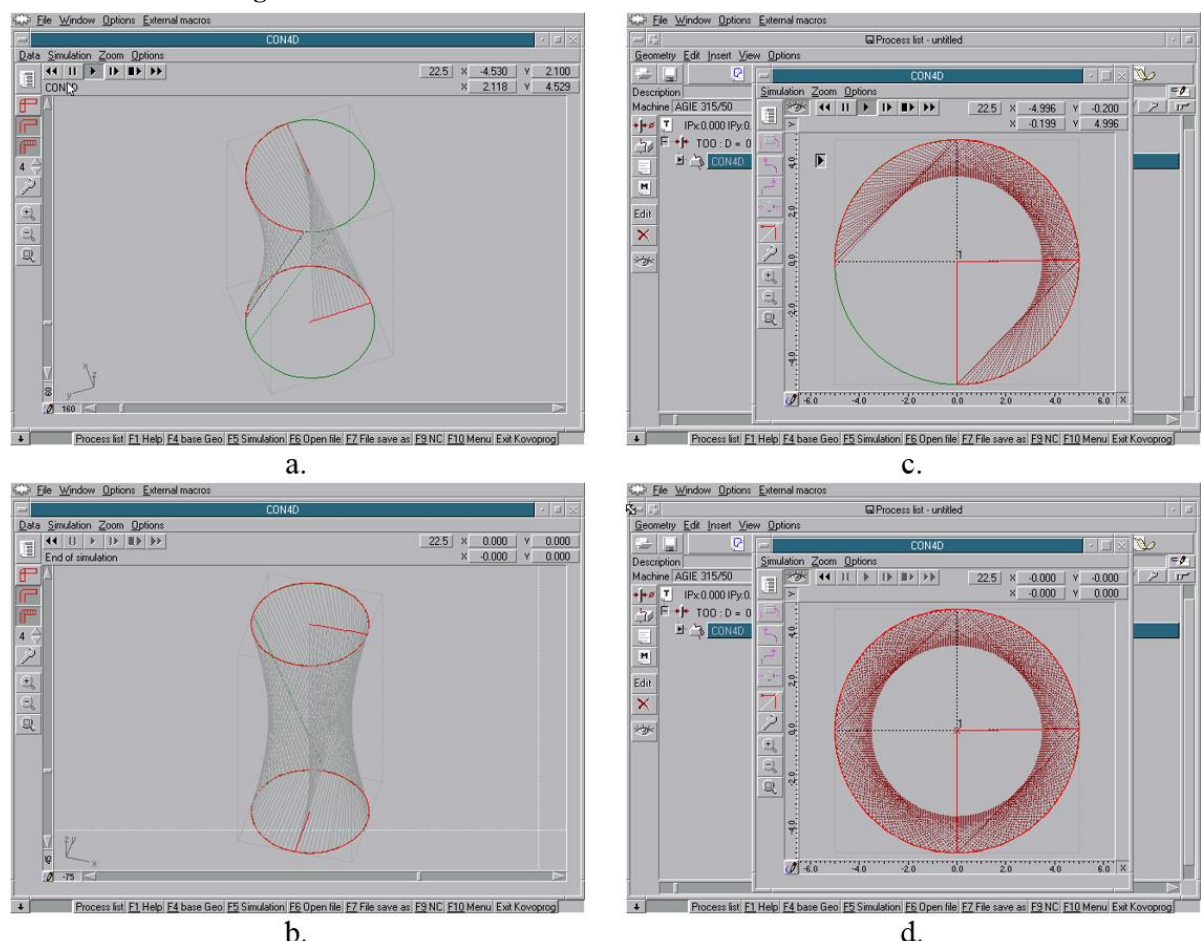


Figure 5. The graphical simulation of the processing of a hyperboloid surface with the aid of the Kovoprog III application

The calculations were made for 9 significant points, assuming the following input data: $r = 15$ mm; $R = 20$ mm; $h = 30$ mm (for which the semiaxes of hyperbola [H] are $a = 15$ mm and $b \approx 34$ mm, according to the notations used in [2]).

It can be noted that the laws of motion of the two endpoints: $M[X, Y]$ and $m_1[x, y]$ can be determined at any point in the processing. The shifts that appear between the sample values of the two points considered are caused by the need to start the processing from point $m_1[x, y]$, offset by displacement angle β (see paper [2]).

The same setup can be graphically simulated using the Kovoprog III application, as can be seen in Figure 5. Sample moments of the processing are presented spatially (Figure 5 a.) and axially projected (Figure 5 b.), together with the result of the processing, which again is illustrated spatially (Figure 5 c.) and axially projected (Figure 5 d.).

The simulation of the hyperboloid surface defined by: $R = 5$, $r = 3.5$ and $H = 22.5$ [mm] was carried out on a machine called AGIE DEM 315. The NC program was created using the Kovoprog III application, and is partially shown in Figure 6 and fully shown in Table 1.

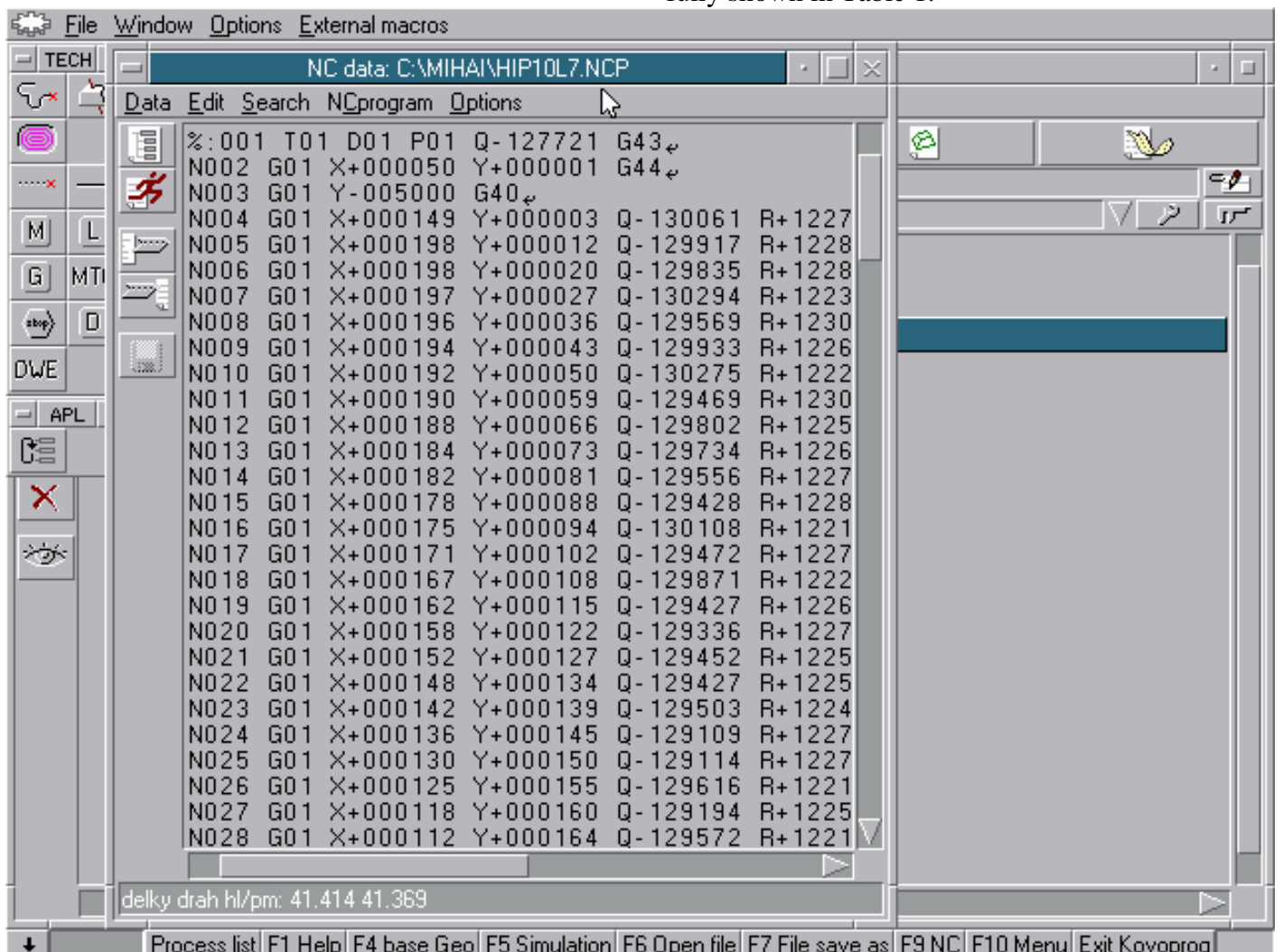


Figure 6. Screen capture of the CN program

This program was then uploaded – using an appropriate interface – to the CNC equipment of the machine, followed by a simulated run to verify its

proper functioning. Having run it, the correct closing of the contour was achieved, as expected.

Table 1. CN program used to generate a hyperboloid surface

%:001 T01 D01 P01 Q-127721 G43	N083 G01 X-000199 Y-000004 Q-127677 R+122870
N002 G01 X+000050 Y+000001 G44	N084 G01 X-000198 Y-000012 Q-127609 R+122938
N003 G01 Y-005000 G40	N085 G01 X-000198 Y-000020 Q-127588 R+122977
N004 G01 X+000149 Y+000003 Q-130061 R+122763	N086 G01 X-000197 Y-000027 Q-128132 R+122448
G42	N087 G01 X-000196 Y-000036 Q-127482 R+123137
N005 G01 X+000198 Y+000012 Q-129917 R+122859	N088 G01 X-000194 Y-000043 Q-127904 R+122721
N006 G01 X+000198 Y+000020 Q-129835 R+122888	N089 G01 X-000192 Y-000050 Q-128320 R+122325
N007 G01 X+000197 Y+000027 Q-130294 R+122353	N090 G01 X-000190 Y-000059 Q-127557 R+123138
N008 G01 X+000196 Y+000036 Q-129569 R+123027	N091 G01 X-000188 Y-000066 Q-127964 R+122715
N009 G01 X+000194 Y+000043 Q-129933 R+122625	N092 G01 X-000184 Y-000073 Q-127964 R+122779
N010 G01 X+000192 Y+000050 Q-130275 R+122208	N093 G01 X-000182 Y-000081 Q-127829 R+122912
N011 G01 X+000190 Y+000059 Q-129469 R+123022	N094 G01 X-000178 Y-000088 Q-127773 R+122989
N012 G01 X+000188 Y+000066 Q-129802 R+122591	N095 G01 X-000175 Y-000094 Q-128546 R+122250
N013 G01 X+000184 Y+000073 Q-129734 R+122648	N096 G01 X-000171 Y-000102 Q-127954 R+122874
N014 G01 X+000182 Y+000081 Q-129556 R+122779	N097 G01 X-000167 Y-000108 Q-128417 R+122418
N015 G01 X+000178 Y+000088 Q-129428 R+122862	N098 G01 X-000162 Y-000115 Q-128032 R+122865
N016 G01 X+000175 Y+000094 Q-130108 R+122100	N099 G01 X-000158 Y-000122 Q-127992 R+122878
N017 G01 X+000171 Y+000102 Q-129472 R+122736	N100 G01 X-000152 Y-000127 Q-128179 R+122736
N018 G01 X+000167 Y+000108 Q-129871 R+122263	N101 G01 X-000148 Y-000134 Q-128219 R+122718
N019 G01 X+000162 Y+000115 Q-129427 R+122697	N102 G01 X-000142 Y-000139 Q-128324 R+122608
N020 G01 X+000158 Y+000122 Q-129336 R+122722	N103 G01 X-000136 Y-000145 Q-128024 R+122969
N021 G01 X+000152 Y+000127 Q-129452 R+122570	N104 G01 X-000130 Y-000150 Q-128088 R+122918
N022 G01 X+000148 Y+000134 Q-129427 R+122537	N105 G01 X-000125 Y-000155 Q-128650 R+122357
N023 G01 X+000142 Y+000139 Q-129503 R+122440	N106 G01 X-000118 Y-000160 Q-128283 R+122781
N024 G01 X+000136 Y+000145 Q-129109 R+122780	N107 G01 X-000112 Y-000164 Q-128736 R+122345
N025 G01 X+000130 Y+000150 Q-129114 R+122733	N108 G01 X-000105 Y-000169 Q-128338 R+122768
N026 G01 X+000125 Y+000155 Q-129616 R+122168	N109 G01 X-000098 Y-000173 Q-128289 R+122862
N027 G01 X+000118 Y+000160 Q-129194 R+122589	N110 G01 X-000091 Y-000176 Q-128495 R+122673
N028 G01 X+000112 Y+000164 Q-129572 R+122153	N111 G01 X-000084 Y-000180 Q-128442 R+122785
N029 G01 X+000105 Y+000169 Q-129137 R+122584	N112 G01 X-000077 Y-000184 Q-128408 R+122832
N030 G01 X+000098 Y+000173 Q-129016 R+122671	N113 G01 X-000070 Y-000186 Q-128851 R+122394
N031 G01 X+000091 Y+000176 Q-129163 R+122490	N114 G01 X-000062 Y-000189 Q-128491 R+122793
N032 G01 X+000084 Y+000180 Q-129043 R+122584	N115 G01 X-000055 Y-000191 Q-128913 R+122388
N033 G01 X+000077 Y+000184 Q-128953 R+122629	N116 G01 X-000047 Y-000193 Q-128731 R+122621
N034 G01 X+000070 Y+000186 Q-129326 R+122214	N117 G01 X-000039 Y-000195 Q-128572 R+122834
N035 G01 X+000062 Y+000189 Q-128936 R+122595	N118 G01 X-000032 Y-000196 Q-129101 R+122317
N036 G01 X+000055 Y+000191 Q-129289 R+122203	N119 G01 X-000023 Y-000198 Q-128362 R+123108
N037 G01 X+000047 Y+000193 Q-129055 R+122416	N120 G01 X-000016 Y-000198 Q-128954 R+122518
N038 G01 X+000039 Y+000195 Q-128828 R+122634	N121 G01 X-000008 Y-000199 Q-128912 R+122594
N039 G01 X+000032 Y+000196 Q-129312 R+122110	N122 G01 Y-000198 Q-128899 R+122665
N040 G01 X+000023 Y+000198 Q-128508 R+122895	N123 G01 X+000008 Y-000199 Q-128889 R+122707
N041 G01 X+000016 Y+000198 Q-129035 R+122316	N124 G01 X+000016 Y-000198 Q-128832 R+122796
N042 G01 X+000008 Y+000199 Q-128928 R+122399	N125 G01 X+000023 Y-000198 Q-129439 R+122184
N043 G01 Y+000198 Q-128874 R+122470	N126 G01 X+000032 Y-000196 Q-128699 R+122991
N044 G01 X-000008 Y+000199 Q-128800 R+122509	N127 G01 X+000039 Y-000195 Q-129250 R+122458
N045 G01 X-000016 Y+000198 Q-128679 R+122589	N128 G01 X+000047 Y-000193 Q-129061 R+122685
N046 G01 X-000023 Y+000198 Q-129219 R+121987	N129 G01 X+000055 Y-000191 Q-128888 R+122910
N047 G01 X-000032 Y+000196 Q-128436 R+122800	N130 G01 X+000062 Y-000189 Q-129299 R+122506
N048 G01 X-000039 Y+000195 Q-128914 R+122291	N131 G01 X+000070 Y-000186 Q-128932 R+122914
N049 G01 X-000047 Y+000193 Q-128684 R+122492	N132 G01 X+000077 Y-000184 Q-129388 R+122473
N050 G01 X-000055 Y+000191 Q-128436 R+122729	N133 G01 X+000084 Y-000180 Q-129363 R+122544
N051 G01 X-000062 Y+000189 Q-128793 R+122340	N134 G01 X+000091 Y-000176 Q-129293 R+122660
N052 G01 X-000070 Y+000186 Q-128379 R+122731	N135 G01 X+000098 Y-000173 Q-129526 R+122473
N053 G01 X-000077 Y+000184 Q-128748 R+122310	N136 G01 X+000105 Y-000169 Q-129467 R+122562
N054 G01 X-000084 Y+000180 Q-128688 R+122388	N137 G01 X+000112 Y-000164 Q-129084 R+122998
N055 G01 X-000091 Y+000176 Q-128548 R+122519	N138 G01 X+000118 Y-000160 Q-129516 R+122580
N056 G01 X-000098 Y+000173 Q-128721 R+122322	N139 G01 X+000125 Y-000155 Q-129134 R+122990
N057 G01 X-000105 Y+000169 Q-128610 R+122428	N140 G01 X+000130 Y-000150 Q-129684 R+122461
N058 G01 X-000112 Y+000164 Q-128152 R+122860	N141 G01 X+000136 Y-000145 Q-129788 R+122414
N059 G01 X-000118 Y+000160 Q-128528 R+122452	N142 G01 X+000142 Y-000139 Q-129475 R+122788
N060 G01 X-000125 Y+000155 Q-128107 R+122876	N143 G01 X+000148 Y-000134 Q-129603 R+122669
N061 G01 X-000130 Y+000150 Q-128595 R+122349	N144 G01 X+000152 Y-000127 Q-129616 R+122680

N062 G01 X-000136 Y+000145 Q-128621 R+122314	N145 G01 X+000158 Y-000122 Q-129804 R+122517
N063 G01 X-000142 Y+000139 Q-128244 R+122671	N146 G01 X+000162 Y-000115 Q-129789 R+122577
N064 G01 X-000148 Y+000134 Q-128306 R+122570	N147 G01 X+000167 Y-000108 Q-129403 R+123004
N065 G01 X-000152 Y+000127 Q-128283 R+122595	N148 G01 X+000171 Y-000102 Q-129856 R+122570
N066 G01 X-000158 Y+000122 Q-128400 R+122440	N149 G01 X+000175 Y-000094 Q-129257 R+123240
N067 G01 X-000162 Y+000115 Q-128324 R+122519	N150 G01 X+000178 Y-000088 Q-130006 R+122486
N068 G01 X-000167 Y+000108 Q-127873 R+122956	N151 G01 X+000182 Y-000081 Q-129964 R+122562
N069 G01 X-000171 Y+000102 Q-128259 R+122536	N152 G01 X+000184 Y-000073 Q-129845 R+122757
N070 G01 X-000175 Y+000094 Q-127598 R+123169	N153 G01 X+000188 Y-000066 Q-129842 R+122785
N071 G01 X-000178 Y+000088 Q-128286 R+122446	N154 G01 X+000190 Y-000059 Q-130261 R+122369
N072 G01 X-000182 Y+000081 Q-128178 R+122536	N155 G01 X+000192 Y-000050 Q-129493 R+123220
N073 G01 X-000184 Y+000073 Q-127989 R+122738	N156 G01 X+000194 Y-000043 Q-129893 R+122834
N074 G01 X-000188 Y+000066 Q-127913 R+122770	N157 G01 X+000196 Y-000036 Q-130314 R+122411
N075 G01 X-000190 Y+000059 Q-128294 R+122397	N158 G01 X+000197 Y-000027 Q-129645 R+123130
N076 G01 X-000192 Y+000050 Q-127444 R+123228	N159 G01 X+000198 Y-000020 Q-130197 R+122589
N077 G01 X-000194 Y+000043 Q-127790 R+122854	N160 G01 X+000198 Y-000012 Q-130168 R+122672
N078 G01 X-000196 Y+000036 Q-128159 R+122463	N161 G01 X+000199 Y-000004 Q-130118 R+122750
N079 G01 X-000197 Y+000027 Q-127426 R+123165	N162 G01 X+001000 Y-000020
N080 G01 X-000198 Y+000020 Q-127893 R+122652	N163 G01 Y+005000 R+000000 G40 M21
N081 G01 X-000198 Y+000012 Q-127821 R+122742	N164 G45 M21 M02
N082 G01 X-000199 Y+000004 Q-127700 R+122823	

3. TECHNOLOGICAL LIMITATIONS CONCERNING THE PROCESSING OF HYPERBOLOID SURFACES

Just like any other technical solution, the processing of hyperboloid surfaces using WEDM also comes with certain technological limitations. These are closely related to the dimensions of the processed surfaces or those of the part that is meant to be processed. Hyperboloid surfaces can be processed via WEDM by using special devices that ensure the controlled revolution of the workpiece or that of the wire electrode, which is to be maintained slanted to the vertical axis.

When processing hyperboloid surfaces by revolving the workpiece, the procedure must be limited to relatively small parts, due to the correlation between the overall dimensions of the workpiece and the maximum opening of the wire guides. Therefore, the revolving workpiece must fit between the wire guides.

Given that the slanting angles of the workpiece must be fulfilled at any moment during the processing depends on a multitude of factors, which makes it difficult to specify the admissible limits. Specific cases can be solved as needed, so as to reach a conclusion concerning the maximum slanting angle under which the workpiece can revolve with relation to the axes of the special device used to angle the workpiece.

When revolving the wire electrode, which is kept angled throughout the processing of the hyperboloid surface, the limitations stem from the fact that the workable hyperboloid surfaces need to be of a lesser height, H , than the maximum opening of the wire

guides, H_{\max} , and the end radius must fit within the confines of the machine's active workspace ($L_1 x L_2$):

$$H = 2 \cdot h \leq H_{\max} \quad (1)$$

$$R \leq \min (L_1 x L_2) \quad (2)$$

An important limitation is given by the displacement angle β , which can be calculated using the relations presented in paper [2]. It can be noticed that when $\beta=0^\circ$, the processed surface is cylindrical, and when $\beta=180^\circ$, the processed surface is split into two coaxial conical surfaces having a common apex. As a consequence, the hyperboloid surfaces that can be processed must have a displacement angle within the field of generation $[0, 180^\circ]$. Since the displacement angle β can be measured either clockwise or anti-clockwise, and since the hyperboloid surface can be processed in either of the above-mentioned directions, the field of generation of the displacement angle will be:

$$\beta \in (-180^\circ, +180^\circ) \quad (3)$$

When processing at an angle $\beta > \pm 180^\circ$ ($\beta < 360^\circ$), we can consider this as a processing carried out under angle β , which is equal to the supplementary angle of the former.

4. CONCLUSIONS

The discrete values of angle β indicate that when using WEDM processing to generate hyperboloid surfaces, this can be treated as having a general character. Particularizing the manufacturing process leads us to the generation of the other surfaces, as schematized in Table 2, based on the notations from Figure 1 (together with the accompanying clarifications).

Table 2. A synthesis of the cases of generation of revolution surfaces using WEDM

Type of surface	Displacement angle	Other relevant dimensions	Remarks
Hyperboloid	$\beta \neq 0^\circ$ $\beta \in (-180^\circ, +180^\circ)$	$R \neq 0, r \neq 0, H \neq 0$	General case
Conical	$\beta = +180^\circ$ or $\beta = -180^\circ$	$R \neq 0, r = 0, H \neq 0$	Specific cases
Cylindrical	$\beta = 0^\circ$	$R = r \neq 0, H \neq 0$	
Planar	$\beta = 0^\circ$ or $\beta \neq 0^\circ$ and $\beta = \text{const.}$	$R = r = \infty, H \neq 0$	

It is worth mentioning that surfaces of a trunk of cone are a particularity of the generation of conical surfaces. Due to this, it can be claimed that Table 2 comprises all the basic revolution surfaces that can be generated when processed via WEDM. Revolution surfaces can be worked by having the axis of the wire electrode travel along a linear trajectory, whereas the generating curve (or curves, if there is more than one generating curve: an upper $[\Delta']$ and a lower $[\Delta]$ one, as shown in Figure 1) is achieved kinematically, via CNC contouring.

The simulations carried out, together with the synthesis of the cases of generation of revolution surfaces using WEDM, attest to the fact that the method proposed by the author to generate

hyperboloid surfaces via WEDM is valid and can be used in practice.

5. REFERENCES

1. Deneș, C. *Contribuții asupra prelucrării prin eroziune electrică cu electrod filiform*. Diss. Universitatea "Lucian Blaga" din Sibiu, Romania, (2002).
2. Deneș, C. *The Processing of Hyperboloid Surfaces using Wire Electrical Discharge Machining – Theoretical Aspects*. The International Conference of Nonconventional Technologies - ICNcT 2018, Timișoara, Romania, (2018).
3. *** *EDM Today*. EDM Publications, Nov.-Dec. 2000.